

## Synthesis of Carbon dot based fluorescent probe for selective and ultrasensitive detection of Hg<sup>2+</sup> in water and living cells

Sasmita Mohapatra<sup>a\*</sup>, Swagatika Sahu,<sup>a</sup> Niharika Sinha,<sup>b</sup> and Sujit K. Bhutia<sup>b</sup>

### Electronic Supplementary Information

#### Experimental

##### Synthesis of N,S Containing Carbon Precursor

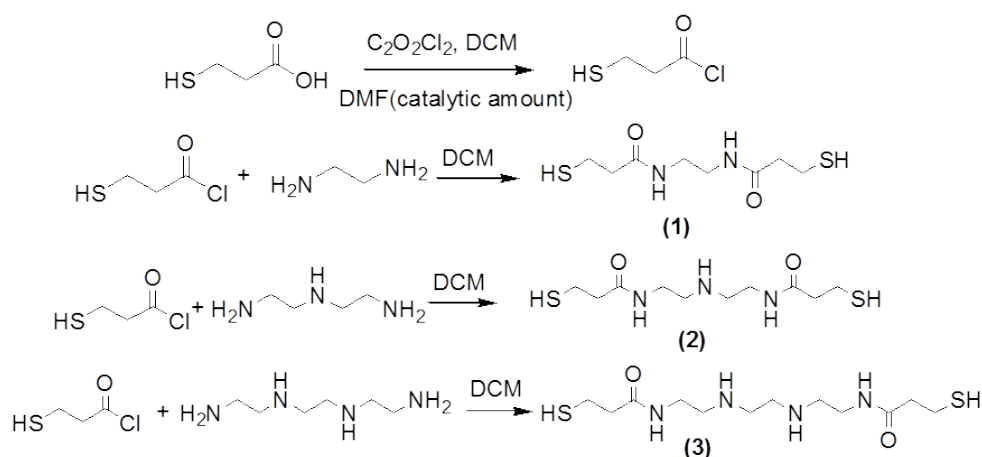
The synthesis of N, S containing carbon precursors has been presented in scheme 1. A solution of 3-mercaptopropionic acid (0.87 mL, 10 mmol) in dichloromethane (5 mL) was cooled to 0 °C under nitrogen. Oxalyl chloride (2 mL, 20 mmol) was added followed by the addition of catalytic amount of DMF. The mixture was allowed to react for 4 h at room temperature. The solvent and unreacted oxalyl chloride was completely removed under vacuum. Then to it ethylenediamine (0.33 mL, 5 mmol) in dichloromethane was added and allowed to react for another 6 h under nitrogen atmosphere. The solid product was recovered through filtration and repeatedly washed with petroleum ether to remove the DMF. Other carbon precursors 2 and 3 with increased N atom were synthesized in similar process by reacting diethylenetriamine (0.53 mL, 5 mmol) and triethylenetetramine (0.75 mL, 5 mmol) respectively instead of ethylenediamine. The compounds are named as 1, 2 and 3, their structures were established by elemental analysis, FTIR, NMR and MS spectral data.

**Carbon precursor 1:** Elemental Analysis: (C 40.2, H 6.92, N 11.9, O 13.51, S 27.13), IR (KBr): 3369, 2973, 2926, 2893, 2742, 2540, 2410, 2139, 1923, 1656, 1451, 1415, 1380, 1328, 1274, 1088, 1048 cm<sup>-1</sup>. <sup>1</sup>H NMR (400 MHz, D<sub>2</sub>O): δ 1.5 (bs, 2H), 2.42 (t, 4H), 2.94 (m, 4H), 3.09 (m, 4H), 8.13 (bs, 2H). MS (ESI): m/z (relative intensity) 275 ([M+K], 90).

**Carbon precursor 2:** Elemental Analysis: (C 42.81, H 7.62, N 14.91, O 11.53, S 23.23) IR (KBr) 3379, 3018, 2966, 2914, 2847, 2706, 2572, 2450, 1727, 1662, 1427, 1368, 1333,

1226, 1215, 1110  $\text{cm}^{-1}$ .  $^1\text{H NMR}$  (400 MHz,  $\text{D}_2\text{O}$ ):  $\delta$  1.5 (bs, 2H,), 2.02 (bs, 1H), 2.3 (t, 4H), 2.92 (m, 8H,), 3.08 (m, 4H), 8.05 (bs, 2H). MS (ESI):  $m/z$  (relative intensity) 314 ( $[\text{M}+\text{N}_2\text{H}_7]$ , 100).

**Carbon precursor 3:** Elemental Analysis: (C 44.52, H 8.34, N 17.4, O 9.81, S 19.8) IR (KBr) 3414, 3018, 2967, 2918, 2840, 2557, 1740, 1640, 1440, 1366, 1323, 1228, 1048  $\text{cm}^{-1}$ .  $^1\text{H NMR}$  (400 MHz,  $\text{D}_2\text{O}$ ):  $\delta$  1.5 (bs, 2H,), 2.0 (bs, 2H), 2.34-2.7 (m, 12H), 2.8-3.32 (m, 8H), 8.0 (bs, 2H). MS (ESI):  $m/z$  (relative intensity) 321 ( $[\text{M}-\text{H}]$ , 84).



Scheme S1 Synthesis of N, S containing precursors

### Fluorescence Quantum yield ( $\Phi$ ) calculation

The quantum yield ( $\Phi$ ) of the synthesized NSCD samples was calculated using quinine sulfate as reference following the our previously reported method.<sup>1</sup> For calculation of quantum yield, five concentrations of each compound were made, all of which had absorbance less than 0.1 nm at 340 nm. Quinine sulfate (literature  $\Phi = 0.54$ ) was dissolved in 0.1 M  $\text{H}_2\text{SO}_4$  (refractive index ( $\eta$ ) of 1.33) while the NSCD samples were dissolved in water ( $\eta = 1.33$ ). Their fluorescence spectra were recorded at same excitation of 340 nm. Then by comparing the integrated photoluminescence intensities (excited at 340 nm) and the absorbency values (at 340 nm) of the carbon sample with the references quinine sulfate quantum yield of the NSCD samples were determined. The quantum yield was calculated using the below equation

$$\Phi_x = \Phi_{\text{ST}} (m_x / m_{\text{ST}}) (\eta_x^2 / \eta_{\text{ST}}^2)$$

Where  $\Phi$  is the quantum yield,  $m$  is slope,  $\eta$  is the refractive index of the solvent,  $ST$  is the standard and  $X$  is the sample.

**Ref:**

- 1 S. Sahu, B. Behera, T. K. Maiti, S. Mohapatra, *Chem. Commun.*, 2012, **48**, 8835-8837.

**Measurement of fluorescence life time**

Time resolved fluorescence decay traces were deconvoluted from the signal and fitted using the FluoFit 4.4 package (Picoquant). The experimental decay traces were fitted to triexponential functions via a Levenberg–Marquardt algorithm based on nonlinear least-squares error minimization deconvolution method. Usually, up to three different exponential terms were used to fit the experimental decay traces. The quality of the fits was judged by the reduced chi-squared method,  $\chi^2$ , the weighted residuals and the correlation functions. The latter two were checked for random distributions. To compare the photoluminescence lifetime of the free carbon dot NSCD and in presence of  $Hg^{2+}$  at different concentrations, it was necessary to determine their average lifetime using eqn:

$$\tau_{avg} = \frac{\sum \alpha_i \tau_i^2}{\sum \alpha_i \tau_i}$$

Where  $\alpha_i$  are the pre-exponential factors and  $\tau_i$  are the lifetimes obtained in the triexponential fitting of the decay curves of carbon dot emission.

**Calculation of detection limit**

All fluorescence emission spectra of the fluorophore were integrated vs. wavenumber, and calibration curves were generated, with the analyte concentration on the X-axis (in nM) and  $F_0/F$  on the Y-axis, where  $F$  = the integrated fluorophore emission at a particular  $Hg^{2+}$  concentration and  $F_0$  = the integrated fluorophore emission in the absence of  $Hg^{2+}$ . The lower Hg concentrations yielded a linear relationship, and the equation for the line was determined. The limit of the blank was taken to be the average of the blank (NSCD emission without  $Hg^{2+}$ ) +30 times the standard deviation of the blank. This value was entered into the equation determined in

(for the Y value), and the corresponding X value was determined. This value provided the LOD in nM.

## Figures

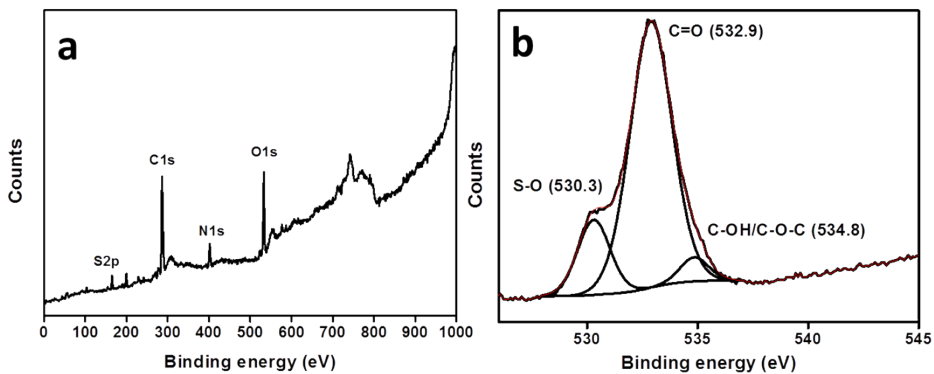


**Fig. S1** (a) XPS survey and (b) high resolution scan of O1s region of NSCD-2.

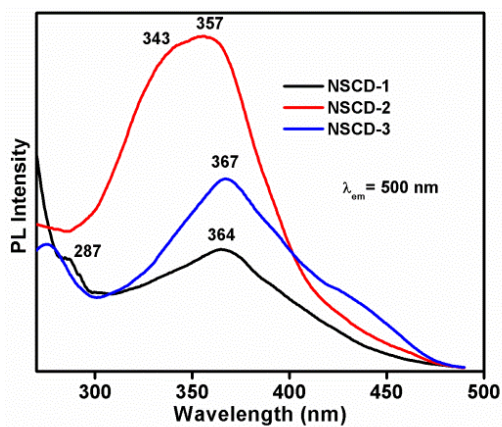


**Fig.S2** Excitation spectra of NSCDs with different nitrogen content.

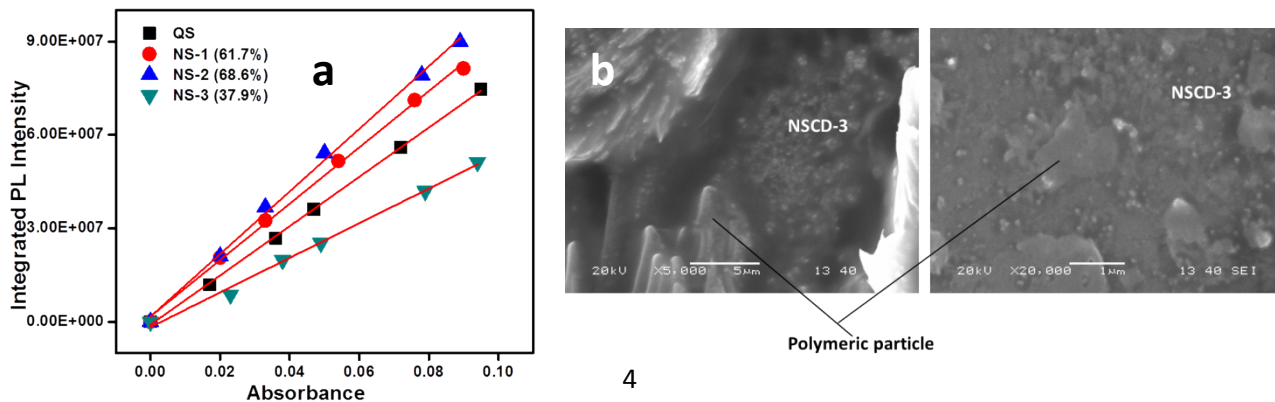


**Fig. S3**(a) Fluorescence and Absorbance of the NSCD and Quinine Sulfate and (b) SEM image of NSCD-3.

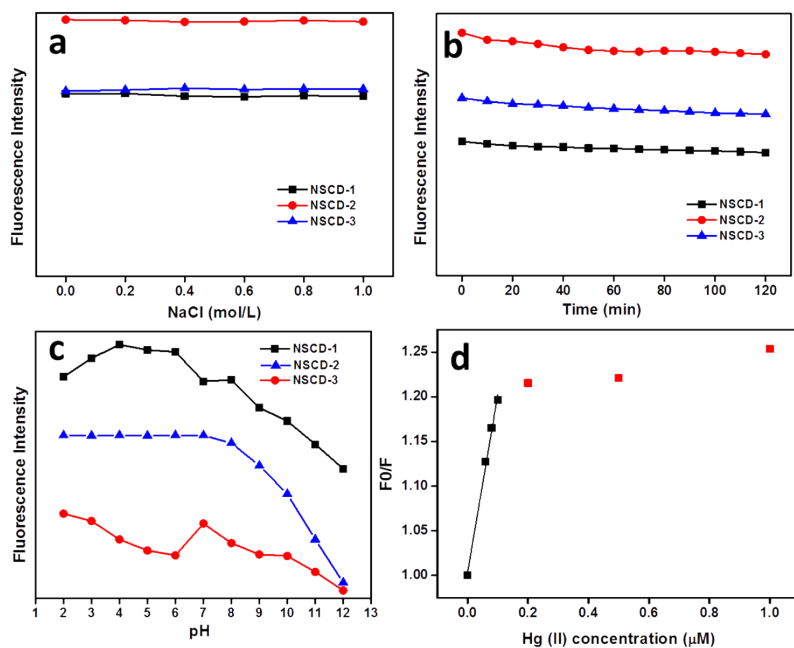


**Fig. S4**(a) Change in fluorescence intensity w.r.t. time, (b) Effect of ionic strengths on the fluorescence intensity of NSCD (ionic strengths were controlled by various concentrations of NaCl), (c) Effect of pH on the fluorescence intensity of NSCD, (d) Linear dependence of fluorescence quenching of NSCD-2 with mercury concentration.

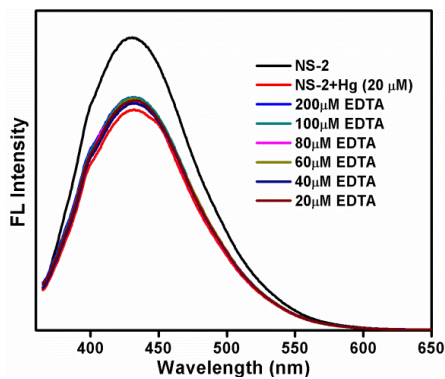


**Fig. S5** Fluorescence response of NSCD-2 after adding EDTA to NSCD-Hg<sup>2+</sup>.

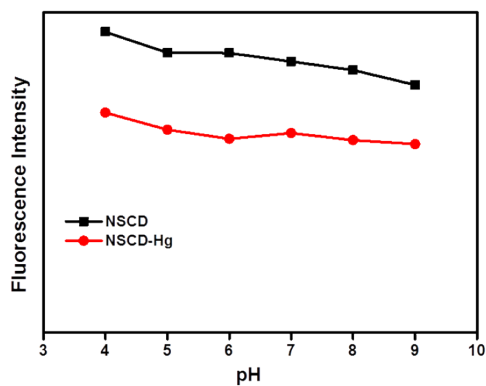


**Fig. S6** Fluorescence quenching of NSCD w.r.t pH

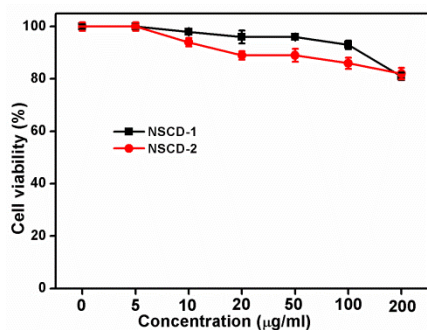


**Fig. S7** Cell viability by MTT assay

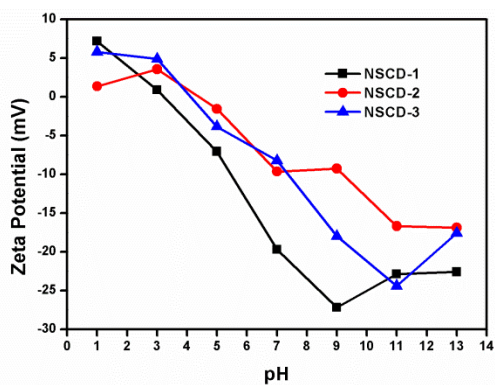


**Fig. S8** Change in zeta potential of NSCD with pH.

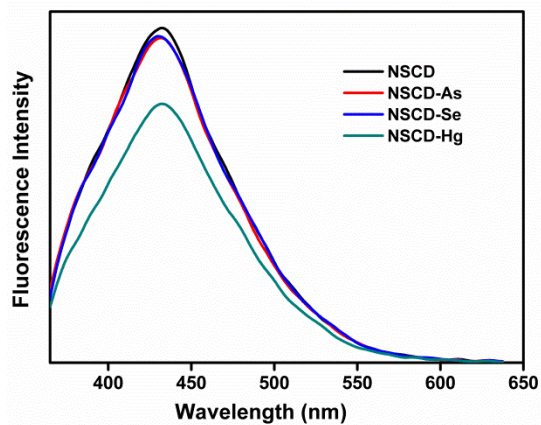
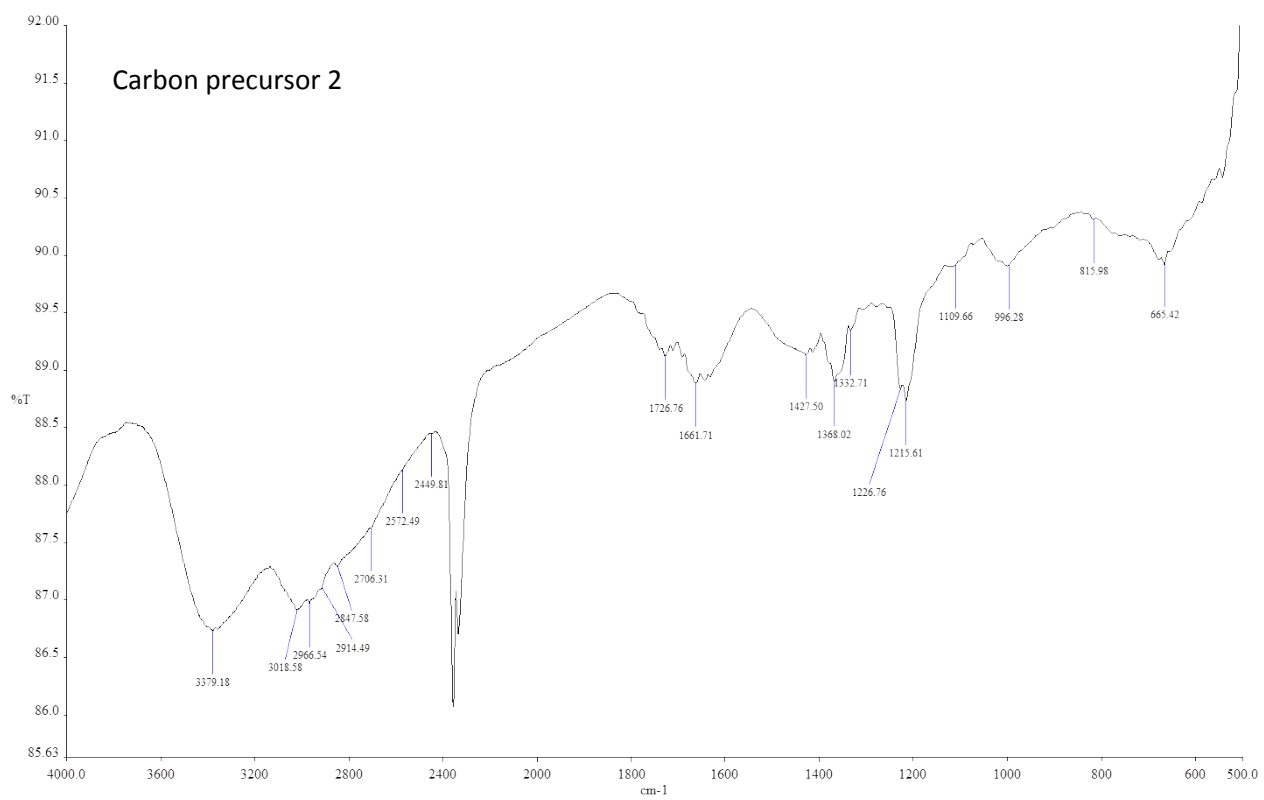
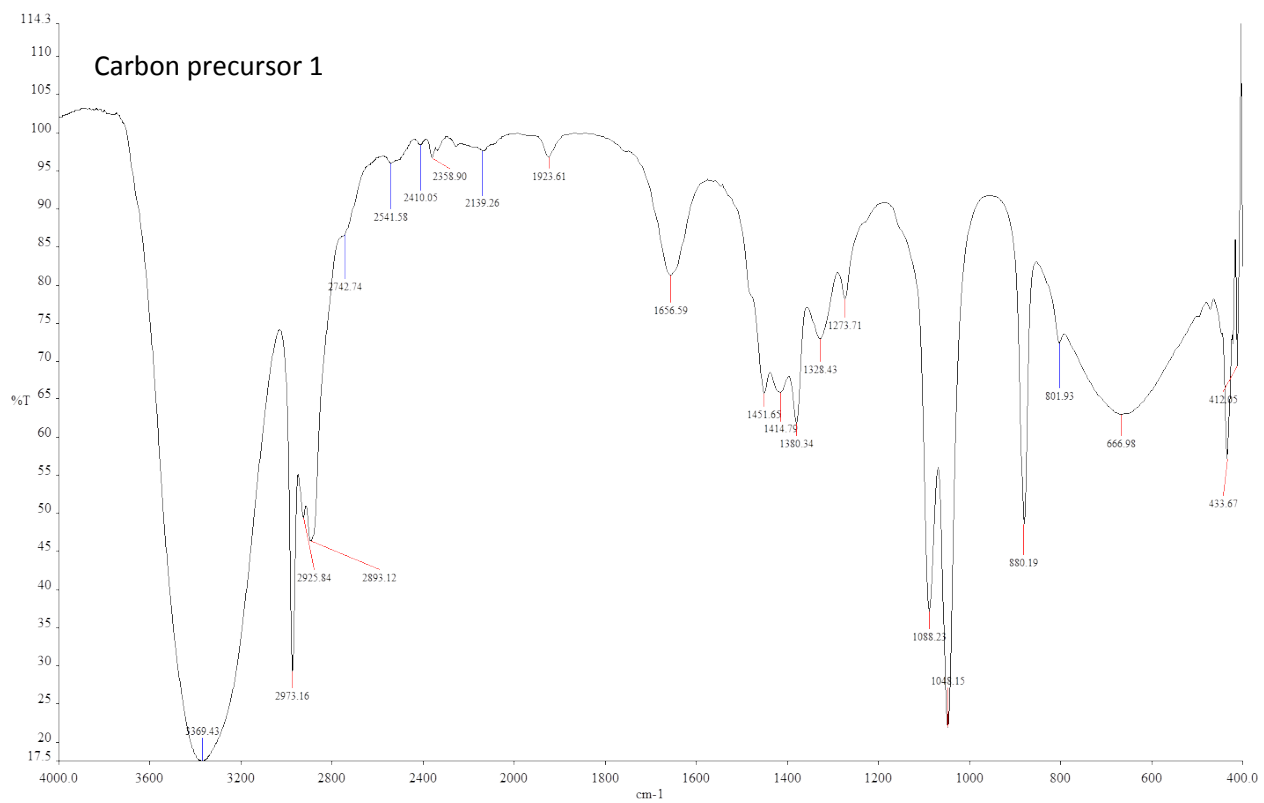


**Fig. S9** Fluorescence quenching of NSCD in the presence of Hg, As and Se metal ions (40 $\mu$ M)

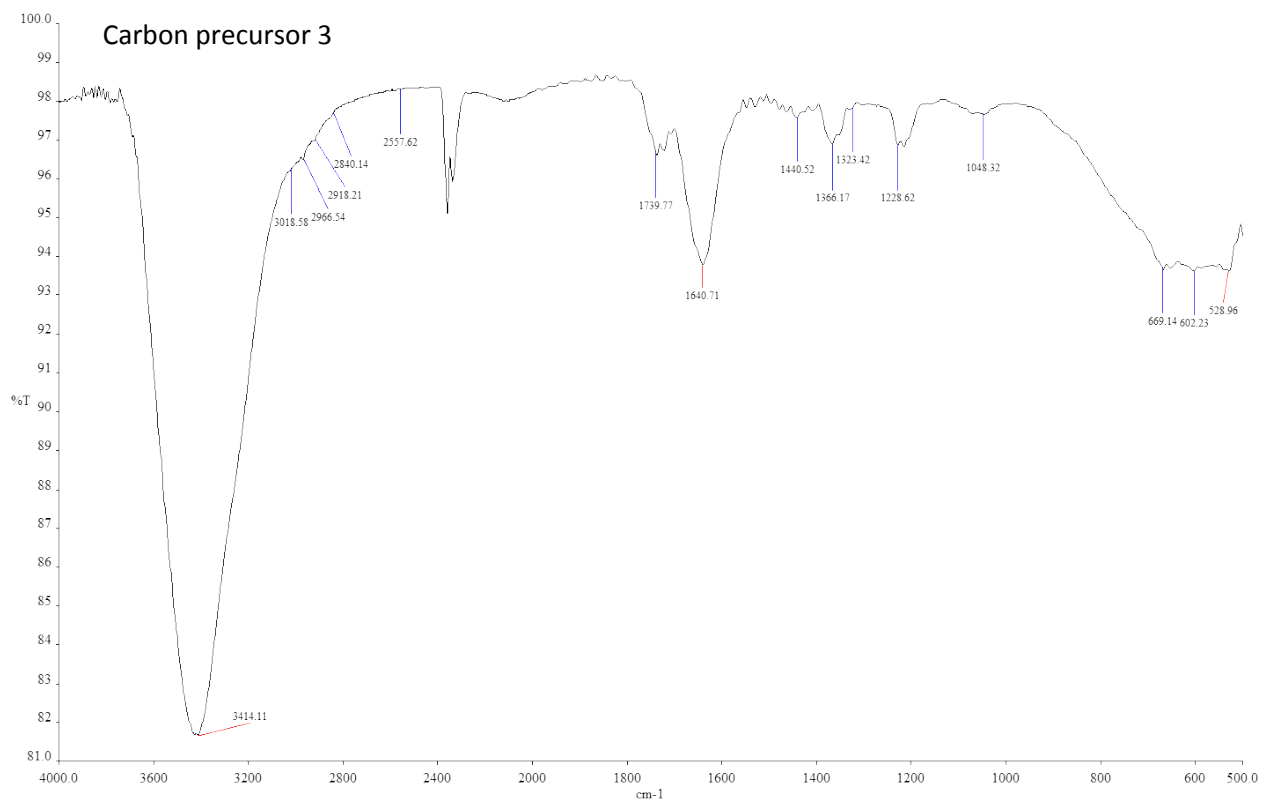
**Table S1** Selectivity coefficients of Hg<sup>2+</sup> over other metal ions

Metal ions	Selectivity coefficients	Metal ions	Selectivity coefficients
Co <sup>2+</sup>	15	Fe <sup>2+</sup>	10
Cu <sup>2+</sup>	-14	Sn <sup>2+</sup>	71
Mn <sup>2+</sup>	21	Zn <sup>2+</sup>	29
Ni <sup>2+</sup>	33	Ca <sup>2+</sup>	38

## IR Spectra







## Mass Spectra

